Solid-State Electronics 54 (2010) 137–142

Contents lists available at ScienceDirect

Solid-State Electronics

journal homepage: www.elsevier.com/locate/sse

Electron subband structure in strained silicon UTB films from the Hensel–Hasegawa–Nakayama model – Part 1 analytical consideration and strain-induced valley splitting

Thomas Windbacher *, Viktor Sverdlov, Oskar Baumgartner, Siegfried Selberherr

Institute for Microelectronics, TU Wien, Gußhausstraße 27-29, 1040 Wien, Austria

A R T I C L E I N F O

Article history:
Received 24 April 2009
Received in revised form 10 June 2009
Accepted 2 September 2009
Available online 31 December 2009

The review of this paper was arranged by Prof. O. Engström

Keywords:
UTB SOI FET
Hensel–Hasegawa–Nakayama **k·p** model
Subband structure

A B S T R A C T

Multi-gate FinFETs and ultra-thin silicon body SOI FETs are considered as perfect candidates for future technology nodes. Strong size quantization leads to a formation of quasi-two-dimensional subbands in carrier systems within thin silicon films. The employed Hensel–Hasegawa–Nakayama **k·p** Hamiltonian accurately describes the bulk structure up to the energies of 0.5–0.8 eV and includes a shear strain component. Shear strain is responsible for effective mass modification and is therefore an important source of the electron mobility enhancement in ultra-thin silicon films. The influence of shear strain on the subband structure in thin silicon films is investigated.

© 2009 Elsevier Ltd. All rights reserved.

1. Introduction

Multi-gate FinFETs and ultra-thin silicon body SOI FETs are considered as perfect candidates for the 22 nm technology node and beyond. Strong size quantization leads to a formation of quasi-two-dimensional subbands in carrier systems within thin silicon films. For analytical hole subband structure calculations a six-band **k·p** Hamiltonian is employed. The electron subband structure consists of six equivalent minima located close to the *X*-points in the Brillouin zone. Close to the minimum the dispersion is usually described by a parabolic approximation with the transversal masses m_t and the longitudinal mass m_l. Isotropic non-parabolicity takes into account deviations in the density of states at higher energies. A more general description is, however, needed in ultra-thin silicon films, especially in presence of shear strain [1]. The two-band **k·p** Hamiltonian accurately describes the bulk structure up to energies of 0.5–0.8 eV [2]. It includes a shear strain component which is neglected in the parabolic approximation [2–4]. Shear strain is responsible for effective mass modification and is therefore an important source of the electron mobility enhancement in ultra-thin silicon films [1,5]. In Part 1 we concentrate on the analytical analysis of the problem, allowing computationally cheap results, while offering already detailed characterization of the UTB silicon films behavior under uniaxially strain. However, the assumption of a square well potential with infinite walls is only valid in a relatively small regime (as long as the ground subband energy is much higher than the amplitude of the potential profile within the film). As soon as this assumption breaks down, a generalized numerical treatment of the **k·p** Schrödinger and Poisson equations is required. This is taken care of in Part 2 [6], where an efficient numerical procedure to obtain the electron subband structure self-consistently is presented, and in this way completes the analysis of uniaxially strained UTB silicon films.

2. Method

The two-band **k·p** Hamiltonian of a [001] valley in the vicinity of the *X*-point of the Brillouin zone in Si must be in the form [3]:

$$H = \left(\frac{\hbar^2 k_z^2}{2m_l} + \frac{\hbar^2\left(k_x^2 + k_y^2\right)}{2m_t} + U(z)\right)I + \left(2\Xi_{u'}\varepsilon_{xy} - \frac{\hbar^2 k_x k_y}{M}\right)\sigma_z + \frac{\hbar^2 k_z k_0}{m_l}\sigma_x \quad (1)$$

where $\sigma_{x,z}$ are the Pauli matrices, I is the 2×2 unity matrix, $k_0 = 0.15 \times 2\pi/a_0$ is the position of the valley minimum relative to the *X*-point in unstrained Si, k_i with $i \in \{x, y, z\}$ is the wave vector,

* Corresponding author.
E-mail addresses: Windbacher@iue.tuwien.ac.at (T. Windbacher), Sverdlov@iue.tuwien.ac.at (V. Sverdlov), Baumgartner@iue.tuwien.ac.at (O. Baumgartner), Selberherr@iue.tuwien.ac.at (S. Selberherr).

0038-1101/$ - see front matter © 2009 Elsevier Ltd. All rights reserved.
doi:10.1016/j.sse.2009.12.008

ε_{xy} denotes the shear strain component in physics notations, $M^{-1} = m_t^{-1} - m_0^{-1}$, and $\Xi_{u'} = 7$ eV is the shear strain deformation potential [2–5].

The confining potential $U(z)$ along the [001] direction modulates the conduction bands profiles. As long as the ground subband energy is much higher than the amplitude of the potential profile within the film, the confining potential in an ultra-thin silicon film can be approximated as square well potential with infinite walls (Fig. 1).

For a square well potential the wave function is set to zero at the boundaries, which allows an analytical analysis of the subband structure.

In the two-band model the wave function is a spinor with two components. Therefore, we use the following ansatz,

$$\psi = \begin{pmatrix} a(\mathbf{k}) \\ b(\mathbf{k}) \end{pmatrix} e^{i\mathbf{k}\cdot\mathbf{r}}, \tag{2}$$

where $a(\mathbf{k})$ and $b(\mathbf{k})$ are coefficients depending on the wave vector $\mathbf{k}$. Substituting this ansatz into the equation system delivers the following eigenvalue problem:

$$(H - E)\begin{pmatrix} a(\mathbf{k}) \\ b(\mathbf{k}) \end{pmatrix} e^{i\mathbf{k}\cdot\mathbf{r}} = 0. \tag{3}$$

Taking the determinant of Eq. (3) and setting it to zero results in the energy dispersion relation of the subband system.

$$E(\mathbf{k}) = \frac{\hbar^2 k_z^2}{2m_l} + \frac{\hbar^2\left(k_x^2 + k_y^2\right)}{2m_t} \pm \sqrt{\delta^2 + \left(\frac{\hbar^2 k_z k_0}{m_l}\right)^2}, \tag{4}$$

with

$$\delta = \left(2\Xi_{u'}\varepsilon_{xy} - \frac{\hbar^2 k_x k_y}{M}\right). \tag{5}$$

For each energy E there are four solutions for k_z (Fig. 2). Fig. 2 shows that $E(\vec{k})$ is even with respect to $k = 0$. Therefore, there are always two independent values k_1 and k_2 for the wave vector, which are complemented to four values by alternating their signs. For energies within the gap two k values are imaginary. The wave function is then a superposition of the solutions with four eigenvectors:

$$\psi(z) = \begin{pmatrix} a(k_1) \\ b(k_1) \end{pmatrix} e^{ik_1\cdot z} + \begin{pmatrix} a(-k_1) \\ b(-k_1) \end{pmatrix} e^{-ik_1\cdot z} + \begin{pmatrix} a(k_2) \\ b(k_2) \end{pmatrix} e^{ik_2\cdot z} + \begin{pmatrix} a(-k_2) \\ b(-k_2) \end{pmatrix} e^{-ik_2\cdot z}. \tag{6}$$

We introduce $c(k)$ as the ratio between $b(k)$ and $a(k)$. $c(k)$ is an odd function with respect to k_z (only k_z is preserved):

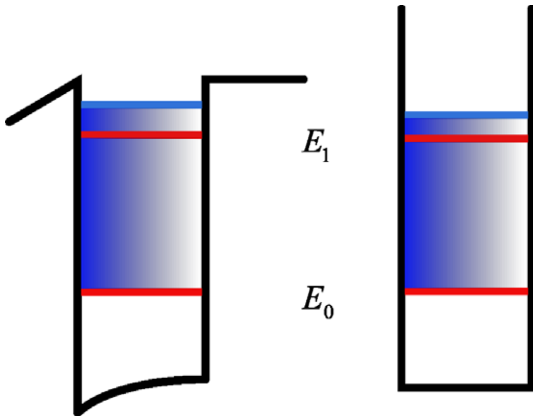

Fig. 1. Potential in an ultra-thin SOI film of a single-gate MOSFET (left) and a corresponding model square well potential with infinite walls.

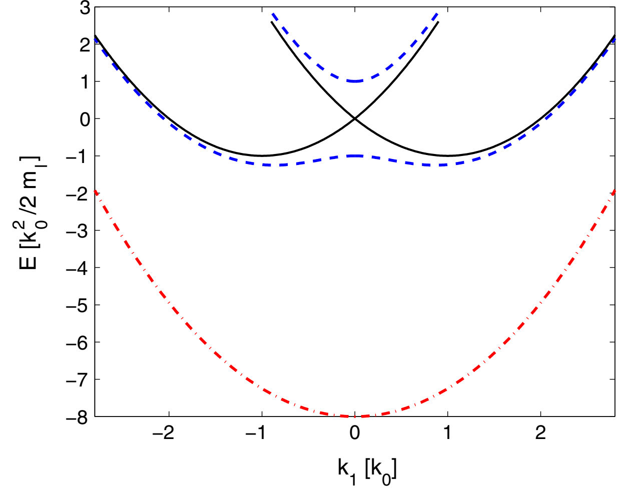

Fig. 2. Conduction band profile close to the X-point for $\eta = 0$ (solid lines, $\eta = 0.5$ (dashed lines), and $\eta = 4$ (dashed-dotted line).

$$c(k_z) = \frac{b(k_z)}{a(k_z)} = -\frac{\frac{\hbar^2 k_z k_0}{m_l}}{\frac{\hbar^2 k_z^2}{2m_l} + \frac{\hbar^2\left(k_x^2 + k_y^2\right)}{2m_t} + \delta - E(k_z)}. \tag{7}$$

Additionally, fulfilling the boundary conditions

$\psi(z = \pm t/2) = 0,$

demands that $a(-k_z) = \pm a(k_z)$ is satisfied. This results in

$$\psi(z) = a(k_1)\left(\begin{pmatrix} 1 \\ c(k_1) \end{pmatrix} e^{ik_1\cdot z} \pm \begin{pmatrix} 1 \\ -c(k_1) \end{pmatrix} e^{-ik_1\cdot z}\right) + a(k_2)\left(\begin{pmatrix} 1 \\ c(k_2) \end{pmatrix} e^{ik_2\cdot z} \pm \begin{pmatrix} 1 \\ -c(k_2) \end{pmatrix} e^{-ik_2\cdot z}\right). \tag{8}$$

After some simplifications the two pairs of independent equations

$$a(k_1)\cos(k_1 t/2) + a(k_2)\cos(k_2 t/2) = 0, \tag{9}$$

$$a(k_1)c(k_1)\sin(k_1 t/2) + a(k_2)c(k_2)\sin(k_2 t/2) = 0, \tag{10}$$

and

$$a(k_1)\sin(k_1 t/2) + a(k_2)\sin(k_2 t/2) = 0, \tag{11}$$

$$a(k_1)c(k_1)\cos(k_1 t/2) + a(k_2)c(k_2)\cos(k_2 t/2) = 0, \tag{12}$$

are obtained. Expressing $a(k_1)$ with Eqs. (9) and (11) and putting them into Eqs. (10) and (12) leads to these two conditions:

$$\tan(k_1 t/2) = \frac{c(k_2)}{c(k_1)}\tan(k_2 t/2), \tag{13}$$

$$\cot(k_1 t/2) = \frac{c(k_2)}{c(k_1)}\cot(k_2 t/2). \tag{14}$$

After transforming the equations into dimensionless form

$$X_{1,2} = \frac{k_{1,2}}{k_0}, \quad E_0 = \frac{\hbar^2 k_0^2}{m_l}, \quad \varepsilon = \frac{E}{E_0}, \quad \eta = \frac{\delta}{E_0}, \tag{15}$$

and few calculation steps found in the Appendix A.1, the equations can be written in the form of:

$$\tan(X_1 k_0 t/2) = \frac{X_2}{X_1}\frac{\eta \pm \sqrt{\eta^2 + X_1^2}}{\eta \pm \sqrt{\eta^2 + X_2^2}}\tan(X_2 k_0 t/2), \tag{16}$$

$$\cot(X_1 k_0 t/2) = \frac{X_2}{X_1}\frac{\eta \pm \sqrt{\eta^2 + X_1^2}}{\eta \pm \sqrt{\eta^2 + X_2^2}}\cot(X_2 k_0 t/2). \tag{17}$$

For solving this equation system it is convenient to reformulate the equations as

$$\sin(X_1 k_0 t/2)\cos(X_2 k_0 t/2) = \frac{X_2}{X_1}\frac{\eta \pm \sqrt{\eta^2 + X_1^2}}{\eta \pm \sqrt{\eta^2 + X_2^2}} \sin(X_2 k_0 t/2) \times \cos(X_1 k_0 t/2), \quad (18)$$

$$\cos(X_1 k_0 t/2)\sin(X_2 k_0 t/2) = \frac{X_2}{X_1}\frac{\eta \pm \sqrt{\eta^2 + X_1^2}}{\eta \pm \sqrt{\eta^2 + X_2^2}} \cos(X_2 k_0 t/2) \times \sin(X_1 k_0 t/2). \quad (19)$$

X_1 and X_2 coexist in the equations. Therefore, we need an extra relation to re-express X_1 as a function of X_2 or vice versa, the derivation of which can be found in the Appendix A.1:

$$X_1^2 = X_2^2 + 4 + 4\sqrt{X_2^2 + \eta^2}, \quad (20)$$

$$X_2^2 = X_1^2 + 4 - 4\sqrt{X_1^2 + \eta^2}. \quad (21)$$

Eliminating one of the two X's with Eq. (20) or Eq. (21) in Eqs. (18) and (19) allows us to calculate X as a function of strain η. Then we can calculate the energy as a function of strain η by using Eq. (4).

3. Results

Interestingly, Eqs. (16) and (17) coincide with the ones obtained from an auxiliary tight-binding consideration [7]. For $\eta = 0$ Eqs. (16) and (17) become equivalent. For higher strain values Eqs. (18) and (19) must be solved numerically. The value $X_2 = \sqrt{X_1^2 + 4 - 4\sqrt{\eta^2 + X_1^2}}$ becomes imaginary at high strain values. In this case the trigonometric functions in Eqs. (16) and (17) or Eqs. (18) and (19) are replaced by the hyperbolic ones. Special care must be taken to choose the correct branch of $\sqrt{X_1^2 + \eta^2}$ in Eqs. (16) and (17) or alternatively Eqs. (18) and (19). The sign of $\sqrt{X_1^2 + \eta^2}$ must be alternated after it becomes zero, as it is displayed in Fig. 3.

Figs. 4 and 5 show the energies of the subbands as a function of shear strain for two different film thicknesses. Shear strain opens the gap between the two conduction bands at the X-point making the dispersions non-parabolic [2], which makes the Eqs. (16) and (17) non-equivalent. This removes the subband degeneracy and introduces the valley splitting. Figs. 6 and 7 show the energy difference between two unprimed subbands ΔE_n as a function of strain for the same quantum number n. We now analyze the limiting cases of Eqs. (16) and (17).

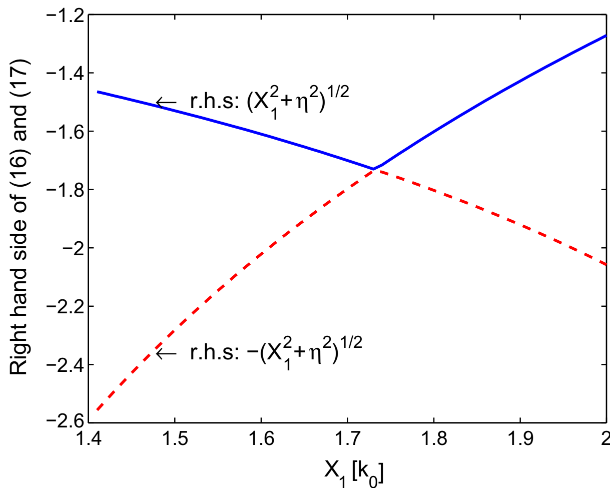

Fig. 3. The right-hand side of Eqs. (16) and (17) plotted close to the point $\sqrt{\eta^2 + X^2} = 0$. It is clearly seen that the sign of the square root must be alternated at this point.

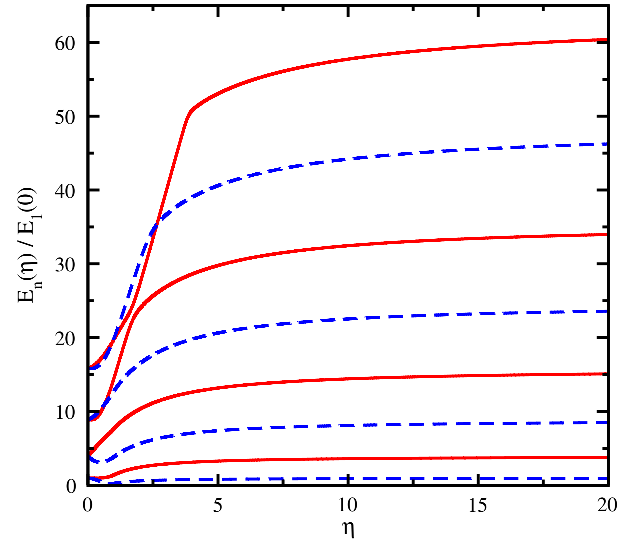

Fig. 4. Subband quantization energies E_n (normalized to the ground subband energy) for a film thickness of 3.3 nm. The valley splitting appears for non-zero shear strain η.

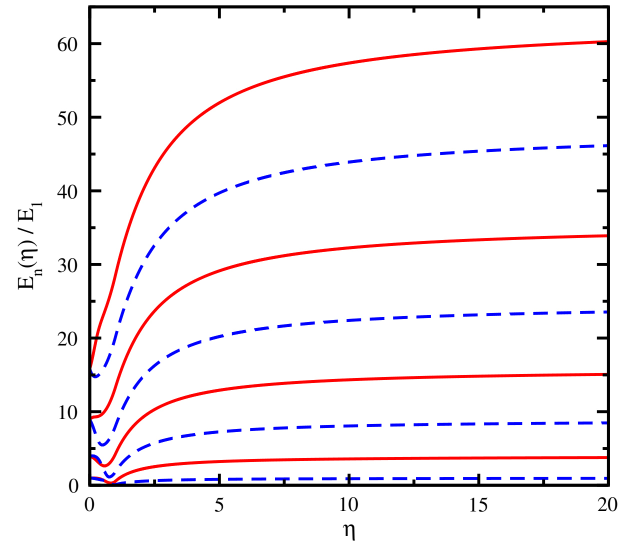

Fig. 5. The same as in Fig. 4 for a film thickness 6.5 nm. The valley splitting depends strongly on the film thickness. The valley splitting is maximal at high strain values.

3.1. Small strain values

The valley splitting was shown to be linear in strain for small shear strain values and to depend strongly on the film thickness [7]. To support these findings we reformulated Eqs. (18) and (19) for the sum and the difference of X_1 and X_2. First we introduce the transformation rules for y_n and $\bar{y}_n$ as,

$$y_n = \frac{X_1 - X_2}{2} \quad \text{and} \quad \bar{y}_n = \frac{X_1 + X_2}{2}, \quad (22)$$

or

$$(y_n + \bar{y}_n)^2 = X_1^2 \quad \text{and} \quad (y_n - \bar{y}_n)^2 = X_2^2. \quad (23)$$

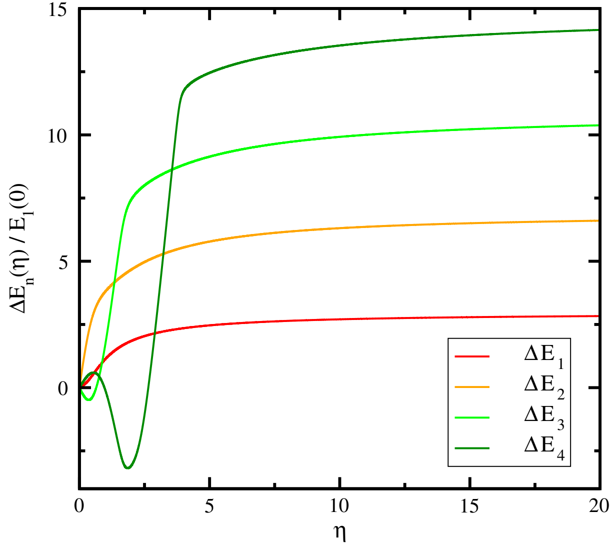

Fig. 6. Difference of the subband quantization energies ΔE_n (normalized to the ground subband energy) from Eqs. (18) and (19) for a film thickness of 3.3 nm. The valley splitting appears for non-zero shear strain η.

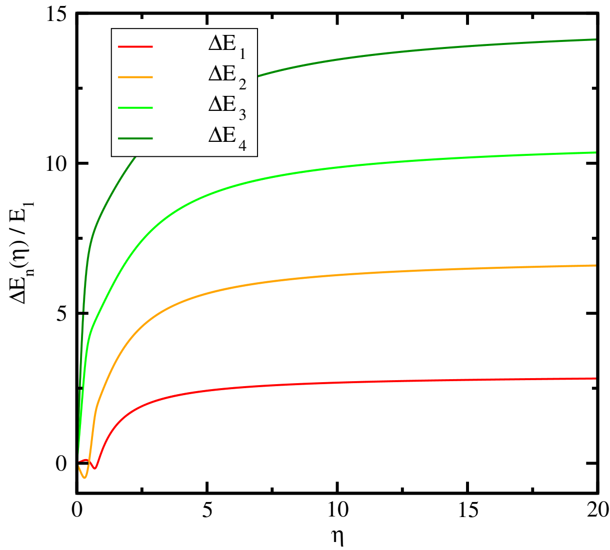

Fig. 7. $\Delta E_n(\eta)$ for a film thickness of 6.5 nm. The splitting depends strongly on the film thickness.

We only show the derivation for Eq. (18), due to the similarity with Eq. (19). Using the above given transformation and rewriting Eq. (18) to separate y_n and $\bar{y}_n$ leads to the following expression.

$$\sin(y_n k_0 t) + \sin(\bar{y}_n k_0 t) = \frac{c(X_2)}{c(X_1)}(-\sin(y_n k_0 t) + \sin(\bar{y}_n k_0 t)). \quad (24)$$

Further simplification steps result in:

$$\sin(y_n k_0 t) = \frac{c(X_2) - c(X_1)}{c(X_2) + c(X_1)} \sin(\bar{y}_n k_0 t). \quad (25)$$

Now we re-express $\bar{y}_n$ as function of y_n (Appendix A.2 resulting in

$$\bar{y}_n^2 = \frac{1 - y_n^2 - \eta^2}{1 - y_n^2}. \quad (26)$$

The derivation of the fraction containing $c(X_1)$ and $c(X_2)$ can be found in Appendix A.2.

$$\sin(y_n k_0 t) = \pm \frac{\eta y_n \sin\left(\sqrt{\frac{1-y_n^2-\eta^2}{1-y_n^2}} k_0 t\right)}{\sqrt{(1-y_n^2)(1-\eta^2-y_n^2)}}. \quad (27)$$

For zero stress the ratio on the right-hand side of Eq. (27) is equal to zero, and the standard quantization condition $q_n = \pi n / k_0 t$ is recovered. Due to the plus/minus sign in the right-hand side of Eq. (27), the equation splits into two non-equivalent branches for $\eta \neq 0$ and non-parabolic bands. Eq. (27) is nonlinear and can be solved only numerically. However, for small η the solution can be sought in the form $y_n = q_n \pm \zeta$, where ζ is small. Substituting $y_n = q_n$ into the right-hand side of Eq. (27) and solving the equation with respect to ζ, we obtain for the valley splitting:

$$\Delta E_n = 4\left(\frac{\pi n}{k_0 t}\right)^2 \frac{\Xi_{u'} \varepsilon_{xy}}{k_0 t} \frac{\sin(k_0 t)}{|1 - q_n^2|}. \quad (28)$$

In accordance with earlier publications [8–10], the valley splitting is inversely proportional to the third power of k_0 and the third power of film thickness t. The value of the valley splitting oscillates with film thickness, in accordance with [9,10]. In contrast to previous works, the subband splitting is proportional to the gap δ at the X-point, and not at the Γ-point. Since the parameter η, which determines non-parabolicity, depends strongly on shear strain, the application of uniaxial [1 1 0] stress to [0 0 1] ultra-thin Si film generates a valley splitting proportional to strain.

3.2. High values of η

For high strain values the dispersion Eq. (4) of the lowest conduction band become parabolic again (shown in Fig. 2) and the quantization levels in a square well potential with a parabolic band must be recovered in this limit. We note that in the limit $\delta \gg E_0 X_2 = 2\sqrt{-\eta}$ and Eqs. (16) and (17) take the form [7]:

$$\tan(X_1 k_0 t/2) \approx \frac{b(X_1)}{a(X_1)} \frac{1}{\sqrt{\eta}}, \quad (29)$$

$$\cot(X_1 k_0 t/2) \approx \frac{b(X_1)}{a(X_1)} \frac{1}{\sqrt{\eta}}. \quad (30)$$

For large η Eq. (29) has the solution $X_1 = \pi(2n-1)/k_0 t$ while Eq. (30) gives $X_1 = 2\pi n / k_0 t$ which results in the well-known quantization result $X_1 = \pi n / k_0 t,\ n = 1, 2, 3, \ldots$ for subbands in an infinite potential square well with a single parabolic band. For the difference in energy ΔE_n between the two subbands degenerate at $\eta = 0$ we get $\Delta E_n = E_1(4n-1)$ in the limit of large η, which is perfectly consistent with the results shown in Figs. 6 and 7.

4. Conclusion

We used the two-band **k·p** model to investigate the subband structure in (0 0 1) silicon films stressed along [1 1 0] direction. It is shown that the unprimed subbands with the same quantum number split for non-zero shear strain. For small strain values the splitting is linear in strain. For large strain the quantization relations in an infinite square well potential with a single parabolic band are recovered resulting in the largest subband splitting. Uniaxial stress is currently used to enhance performance of modern MOSFETs, where it is introduced in a controllable way. Therefore, the valley splitting can be controlled by adjusting strain and thickness t.

The approximation of the confinement potential by the square well potential with infinite walls is valid in ultra-thin body films as long as the ground subband energy is much higher than the amplitude of the potential profile within the film. With the film thickness increased this approximation breaks down in both single- and double-gate UTB structures at higher carrier

concentrations/gate voltages, and a generalized numerical treatment of the **k·p** Schrödinger and Poisson equations is required. An efficient numerical procedure to obtain the electron subband structure self-consistently is described in detail in Part 2 of the paper [6].

Acknowledgment

This work was supported in part by the Austrian Science Fund FWF, Project P19997-N14.

Appendix A

A.1. Re-expressing X_1 as a function of X_2

In the first step the Hamiltonian Eq. (1) and the energy dispersion Eq. (4) are transformed to dimensionless units with the given expressions.

$$X = \frac{k_z}{k_0}, \quad E_0 = \frac{\hbar^2 k_0^2}{m_l}, \quad \varepsilon = \frac{E}{E_0}, \quad \eta = \frac{\delta}{E_0}. \tag{31}$$

The energy dispersion then takes the following form:

$$\varepsilon(X) = \frac{X^2}{2} \pm \sqrt{\eta^2 + X^2} + \frac{m_l\left(k_x^2 + k_y^2\right)}{2 m_t k_0^2}. \tag{32}$$

Setting the determinant of the dimensionless Hamiltonian to zero allows to express X as a function of energy ε:

$$\left(\frac{X^2}{2} - X - \varepsilon\right)\left(\frac{X^2}{2} + X - \varepsilon\right) - \eta^2 = 0$$
$$\text{or} \quad \left(\frac{X^2}{2} - \varepsilon\right)^2 - X^2 - \eta^2 = 0. \tag{33}$$

Re-expressing the fourth order Eq. (33) as second order equation $\frac{\xi^2}{4} - \xi\varepsilon + \varepsilon^2 - \xi - \eta^2 = 0$ by

$$\xi = X^2, \tag{34}$$

we find the solution,

$$\xi = 2(1+\varepsilon) \pm \sqrt{4(1+\varepsilon)^2 - 4(\varepsilon^2 - \eta^2)} \text{ or}$$
$$\xi = 2(1+\varepsilon) \pm 2\sqrt{1 + 2\varepsilon + \eta^2}, \tag{35}$$

preserves all four solutions of X. Embracing two sets of X values in two separate equations leads to the following equations:

$$\xi = \left(1 \pm \sqrt{1 + 2\varepsilon + \eta^2}\right)^2 - \eta^2, \tag{36}$$

$$X_1^2 = \left(1 + \sqrt{1 + 2\varepsilon + \eta^2}\right)^2 - \eta^2, \tag{37}$$

$$X_2^2 = \left(1 - \sqrt{1 + 2\varepsilon + \eta^2}\right)^2 - \eta^2. \tag{38}$$

Using the identities:

$$\frac{X_1^2 + X_2^2}{2} = 2(1+\varepsilon), \tag{39}$$

$$\frac{X_1^2 - X_2^2}{2} = 2\sqrt{1 + 2\varepsilon + \eta^2}, \tag{40}$$

leads to the desired expressions $X_1(X_2)$ and $X_2(X_1)$:

$$X_1^2 = \left(1 + \frac{X_1^2 - X_2^2}{4}\right)^2 - \eta^2, \tag{41}$$

$$X_2^2 = \left(1 - \frac{X_1^2 - X_2^2}{4}\right)^2 - \eta^2 \text{ or} \tag{42}$$

$$X_1^2 = X_2^2 + 4 + 4\sqrt{X_2^2 + \eta^2}, \tag{43}$$

$$X_2^2 = X_1^2 + 4 - 4\sqrt{X_1^2 + \eta^2}. \tag{44}$$

The transformation to dimensionless units completes the corresponding expression for $c(X)$:

$$c(X) = -\frac{X}{\eta \pm \sqrt{\eta^2 + X^2}}. \tag{45}$$

A.2. Expressing the equations as differences

In order to rewrite Eq. (24) as a function of y_n the following set of rules is needed:

$$(\bar{y}_n + y_n) = X_1, \tag{46}$$
$$(\bar{y}_n - y_n) = X_2, \tag{47}$$

or

$$\frac{X_1 + X_2}{2} = y_n, \tag{48}$$
$$\frac{X_1 - X_2}{2} = \bar{y}_n. \tag{49}$$

The following identities (Eqs. (41) and (42)):

$$(\bar{y}_n \pm y_n)^2 + \eta^2 = \left(1 \pm \frac{X_1^2 - X_2^2}{4}\right)^2, \tag{50}$$

$$\bar{y}_n^2 + y_n^2 + \eta^2 = 1 + \frac{X_1^2 - X_2^2}{4}, \tag{51}$$

$$\bar{y}_n y_n = \frac{X_1^2 - X_2^2}{4}, \tag{52}$$

allow to write $\bar{y}_n$ as function of y_n,

$$\bar{y}_n^2 + y_n^2 + \eta^2 = 1 + \bar{y}_n^2 y_n^2, \tag{53}$$
$$\bar{y}_n^2(1 - y_n^2) = 1 - y_n^2 - \eta^2, \tag{54}$$
$$\bar{y}_n^2 = \frac{1 - y_n^2 - \eta^2}{1 - y_n^2}, \tag{55}$$

and y_n as function of $\bar{y}_n$,

$$\bar{y}_n^2 + y_n^2 + \eta^2 = 1 + \bar{y}_n^2 y_n^2, \tag{56}$$
$$y_n^2(1 - \bar{y}_n^2) = 1 - \bar{y}_n^2 - \eta^2, \tag{57}$$
$$y_n^2 = \frac{1 - \bar{y}_n^2 - \eta^2}{1 - \bar{y}_n^2}. \tag{58}$$

Starting with the fraction of Eq. (25) in dimensionless form $I \equiv \frac{c(X_2) - c(X_1)}{c(X_2) + c(X_1)}$, and putting in the definition of $c(X)$, leads to the term below:

$$I \equiv \frac{X_2\left(\eta \pm \sqrt{\eta^2 + X_1^2}\right) - X_1\left(\eta \pm \sqrt{\eta^2 + X_2^2}\right)}{X_2\left(\eta \pm \sqrt{\eta^2 + X_1^2}\right) + X_1\left(\eta \pm \sqrt{\eta^2 + X_2^2}\right)}. \tag{59}$$

Proceeding by substituting X_1 with Eq. (46) and X_2 with Eq. (47), and using the identity $\sqrt{X_{1,2}^2 + \eta^2} = \left|1 \pm \frac{X_1^2 - X_2^2}{4}\right| = |1 \pm \bar{y}_n y_n|$, the term can be rewriting as a function of $\bar{y}_n$ and y_n,

$$I \equiv \frac{(\bar{y}_n - y_n)(\eta \pm (1 + \bar{y}_n y_n)) - (\bar{y}_n + y_n)(\eta \pm (1 - \bar{y}_n y_n))}{(\bar{y}_n - y_n)(\eta \pm (1 + \bar{y}_n y_n)) + (\bar{y}_n + y_n)(\eta \pm (1 - \bar{y}_n y_n))}, \quad (60)$$

Expanding the brackets and reorganizing the expression results in:

$$I \equiv -\frac{y_n(\eta \pm 1 \mp \bar{y}_n^2)}{\bar{y}_n(\eta \pm 1 \mp y_n^2)}. \quad (61)$$

After substituting $\sqrt{\frac{1-y_n^2-\eta^2}{1-y_n^2}}$ for $\bar{y}_n$ the expression simplifies to:

$$I \equiv \frac{-y_n\eta\left(1 \pm \frac{\eta}{1-y_n^2}\right)}{(\eta \pm 1 \mp y_n^2)\sqrt{\frac{1-y_n^2-\eta^2}{1-y_n^2}}}, \quad (62)$$

and can be reformulated to the term used in Eq. (26):

$$I \equiv \mp \frac{y_n\eta}{\sqrt{(1-y_n^2)(1-y_n^2-\eta^2)}}. \quad (63)$$

References

[1] Uchida K, Kinoshita A, Saitoh M. Carrier transport in (110) nMOSFETs: subband structures, non-parabolicity, mobility characteristics, and uniaxial stress engineering. In: IEDM techn dig; 2006. p. 1019–21.

[2] Sverdlov V, Ungersboeck E, Kosina H, Selberherr S. Effects of shear strain on the conduction band in silicon: an efficient two-band **k·p** theory. In: Proc ESSDRC, München; 2007. p. 386–9.

[3] Bir G, Pikus G. Symmetry and strain-induced effects in semiconductors. New York/Toronto: J. Wiley & Sons; 1974.

[4] Hensel JC, Hasegawa H, Nakayama M. Cyclotron resonance in uniaxially stressed silicon. II. Nature of the covalent bond. Phys Rev 1965;138(1A):A225–38. doi:10.1103/PhysRev.138.A225.

[5] Ungersboeck E, Dhar S, Karlowatz G, Sverdlov V, Kosina H, Selberherr S. The effect of general strain on the band structure and electron mobility of silicon. IEEE Trans Electron Dev 2007;54(9):2183–90.

[6] Baumgartner O, Karner M, Sverdlov V, Kosina H. Electron subband structure in strained silicon UTB films from the Hensel–Hasegawa–Nakayama model – part 2: efficient self-consistent numerical solution of the **k·p** Schrödinger equation. Solid-State Electron 2010;54(2):143–8.

[7] Sverdlov V, Selberherr S. Electron subband structure and controlled valley splitting in silicon thin-body SOI FETs: two-band **k·p** theory and beyond. Solid State Electron 2008;52(12):1861–6.

[8] Ando T, Fowler AB, Stern F. Electronic properties of two-dimensional systems. Rev Mod Phys 1982;54(2):437–672. doi:10.1103/RevModPhys.54.437.

[9] Boykin Timothy B, Klimeck Gerhard, Oyafuso Fabiano. Valence band effective – mass expressions in the $sp^3d^5s^*$ empirical tight-binding model applied to a Si and Ge parametrization. Phys Rev B (Condensed Matter Mater Phys) 2004;69(11):115201. doi:10.1103/PhysRevB.69.115201.

[10] Esseni D, Palestri P. Linear combination of bulk bands method for investigating the low-dimensional electron gas in nanostructured devices. Phys Rev B 2005;72(16):165342. doi:10.1103/PhysRevB.72.165342.